Use of Photolithography to Encode Cell Adhesive Domains into Protein Microarrays

Ji Youn Lee,[†] Sunny S. Shah,[†] Christopher C. Zimmer,[‡] Gang-yu Liu,[‡] and Alexander Revzin*,[†]

Departments of Biomedical Engineering and Chemistry, University of California, Davis, Davis, California 95616

Received September 17, 2007. In Final Form: November 5, 2007

Protein microarrays are rapidly emerging as valuable tools in creating combinatorial cell culture systems where inducers of cellular differentiation can be identified in a rapid and multiplexed fashion. In the present study, protein microarraying was combined with photoresist lithography to enable printing of extracellular matrix (ECM) protein arrays while precisely controlling "on-the-spot" cell−cell interactions. In this surface engineering approach, the micropatterned photoresist layer formed on a glass substrate served as a temporary stencil during the microarray printing, defining the micrometer-scale dimensions and the geometry of the cell-adhesion domains within the printed protein spots. After removal of the photoresist, the glass substrates contained micrometer-scale cell-adhesive regions that were encoded within 300 or 500 μm diameter protein domains. Fluorescence microscopy and atomic force microscopy (AFM) were employed to characterize protein micropatterns. When incubated with micropatterned surfaces, hepatic (HepG2) cells attached on 300 or 500 μm diameter protein spots; however, the extent of cell−cell contacts within each spot varied in accordance with dimensions of the photoresist stencil, from single cells attaching on 30 μm diameter features to multicell clusters residing on 100 or 200 μm diameter regions. Importantly, the photoresist removal process was shown to have no detrimental effects on the ability of several ECM proteins (collagens I, II, and IV and laminin) to support functional hepatic cultures. The micropatterning approach described here allows for a small cell population seeded onto a single cell culture substrate to be exposed to multiple scenarios of cell−cell and cell−surface interactions in parallel. This technology will be particularly useful for high-throughput screening of biological stimuli required for tissue specification of stem cells or for maintenance of differentiated phenotype in scarce primary cells.

Introduction

The local microenvironment consisting of neighboring cells, extracellular matrix (ECM) components, and soluble factors has been implicated as a regulator of tissue differentiation and morphogenesis.[1−3] Understanding how components of microenvironment converge to drive and maintain a certain cell phenotype is central for induction of tissue specification in stem cells or for maintenance of differentiated function in primary cells. Recently, attention has turned to miniaturization and multiplexing of cell−microenvironment interactions in order to expedite the discovery of biological stimuli of cell differentiation and to minimize the cost of expensive cells or reagents.[4−7]

Micropatterning approaches have been used extensively as a means of creating a well-defined local microenvironment for the in vitro study of cellular interactions.[8−12] In one of the early studies employing microfabrication approaches, Singhvi et al.[13] precisely defined cell−cell interactions of primary hepatocytes cultured on gold surfaces using principles of microcontact printing, alkanethiol self-assembly, and protein micropatterning. Other soft lithography techniques have been used widely for simulating cell−matrix interactions through patterning of ECM proteins and interrogating the effects of soluble factors through microfluidics.[14−16] In addition to soft lithography, traditional photoresist lithography[17,18] and other photolithography-derived procedures[19−21] have been employed for creating protein micropatterns and designing cellular interactions. While offering precise control over the cell−cell contacts, most surface micropatterning approaches are not suitable for presenting multiple biomolecules on the same surface for multiplexed screening of cell−surface interactions.

* Corresponding author: Department of Biomedical Engineering, University of California, Davis, 451 East Health Sciences St. #2619, Davis, CA 95616; e-mail: arevzin@ucdavis.edu; phone 530-752-2383.

[†] Department of Biomedical Engineering.

[‡] Department of Chemistry.

(1) Bissell, M. J.; Hall, H. G.; Parry, G. *J. Theor. Biol.* **1982**, *99*, 31−68.
(2) Takeichi, M. *Curr. Opin. Cell Biol.* **1995**, *7*, 619−627.
(3) Frisch, S. M.; Francis, H. *J. Cell Biol.* **1994**, *124*, 619−626.
(4) El-Ali, J.; Sorger, P. K.; Jensen, K. F. *Nature* **2006**, *442*, 403−411.
(5) Anderson, D. G.; Levenberg, S.; Langer, R. *Nat. Biotechnol.* **2004**, *22*, 863−866.
(6) Flaim, C. J.; Chien, S.; Bhatia, S. N. *Nat. Methods* **2005**, *3*, 119.
(7) Ding, S.; Schultz, P. G. *Nat. Biotechnol.* **2004**, *22*, 833−849.
(8) Folch, A.; Toner, M. *Annu. Rev. Biomed. Eng.* ***2000***, 2, 227.
(9) Park, T. H.; Shuler, M. L. *Biotechnol. Prog.* **2003**, *19*, 243−253.
(10) Whitesides, G. M.; Ostuni, E.; Takayama, S.; Jiang, X.; Ingber, D. E. *Annu. Rev. Biomed. Eng.* **2001**, *3*, 335−373.
(11) Falconnet, D.; Csucs, G.; Grandin, H. M.; Textor, M. *Biomaterials* **2006**, *27*, 3044−63.
(12) Khademhosseini, A.; Langer, R.; Borenstein, J.; Vacanti, J. P. *Proc. Natl. Acad. Sci. U.S.A.* **2006**, *103*, 2480−2487.
(13) Singhvi, R.; Kumar, A.; Lopez, G. P.; Stephanopoulos, G. N.; Wang, D. I.; Whitesides, G. M.; Ingber, D. E. *Science* **1994**, *264*, 696−698.
(14) Kane, R. S.; Takayma, S.; Ostuni, E.; Ingber, D. E.; Whitesides, G. M. *Biomaterials* **1999**, *20*, 2363−2376.
(15) Takayama, S.; McDonald, J. C.; Ostuni, E.; Liang, M. N.; Kenis, P. J. A.; Ismagilov, R. F.; Whitesides, G. M. *Proc. Natl. Acad. Sci. U.S.A.* **1999**, *96*, 5545−5548.
(16) Jeon, N. L.; Baskaran, H.; Detringer, S. K. W.; Whitesides, G. M.; Van, de Water, L.; Toner, M. *Nat. Biotechnol.* **2002**, *20*, 826−830.
(17) Lom, B.; Healy, K. E.; Hockberger, P. E. *J. Neurosci. Methods* **1993**, *50* (3), 385−397.
(18) Bhatia, S. N.; Yarmush, M. L.; Toner, M. *J. Biomed. Mater. Res.* **1997**, *34*, 189−199.
(19) Dulcey, C. S.; Georger, J. H.; Krauthamer, V.; Stenger, D. A.; Fare, T. L.; Calvert, J. M. *Science* **1991**, *252*, 551−554.
(20) Revzin, A.; Tompkins, R. G.; Toner, M. *Langmuir* **2003**, *19*, 9855−9862.
(21) Revzin, A.; Russell, R. J.; Yadavalli, V. K.; Koh, W.-G.; Deister, C.; Hile, D. D.; Mellott, M. B.; Pishko, M. V. *Langmuir* **2001**, *17*, 5440−5447.

10.1021/la702883d CCC: $40.75 © 2008 American Chemical Society
Published on Web 01/17/2008

In contrast, the microarray printing technology was developed with multiplexing in mind and was originally employed for high-throughput screening of DNA hybridization events.[22] More recently this technology has been adapted to printing arrays of small molecules, biomaterials, or ECM proteins for high-throughput investigation of cell−substrate interactions.[5−7,23] While atomic force microscopy (AFM) and microfabrication technologies have been employed to create nanometer-scale (200−500 nm diameter) array spots,[24,25] commercial robotic printers construct arrays consisting of 100−500 μm diameter spots. The printed spots are typically circular, with spot diameter depending largely on the dimensions of the printing pin, surface wettability, and viscocity of the printing solution. Recently, the use of a temporary microfabricated stencil was proposed as a method for controlling dimensions and improving morphology of printed DNA microarrays.[26]

While robotically printed microarrays show considerable promise as tools for high-throughput screening of cell−substrate interactions,[5−7,23] "on-the-spot" intercellular contacts are poorly defined, resulting in formation of relatively large cell clusters corresponding to the dimensions of the printed spots. The cellular interactions by juxtacrine (cell−cell contact) or endocrine mechanisms are important in tissue morphogenesis, stem cell lineage selection, and maintenance of differentiated cell phenotype.[2,27−29] The ability to precisely define and vary cell−cell contacts occurring on printed protein arrays would allow to control another important biological stimulus in a high-throughput investigation of cell−microenvironment interactions.

Our goal was to develop a surface micropatterning approach that retains multiplexing capabilities offered by protein microarraying but introduces precise control over the extent of cell−cell interactions occurring on printed protein domains. In order to decouple the area of a cell-attachment site from the dimensions of a spotted protein domain, the microarrays were printed onto glass slides containing a micropatterned photoresist layer. Upon removal of the photoresist, 300 or 500 μm diameter protein spots became encoded with cell-adhesive sites ranging in dimensions from 30 to 200 μm diameter. Upon incubation with the micropatterned protein arrays, hepatic (HepG2) cells attached onto 300 or 500 μm protein (typically collagen I) spots; however, the distribution of cells within a protein spot ranged from single cells attaching on 30 μm diameter features to multicell clusters residing on 50, 100, and 200 μm diameter regions. Incubating hepatic cell patterns with 3T3 fibroblasts resulted in formation complex hepatocellular microenvironment incorporating hepatocyte−surface, hepatocyte−hepatocyte, and hepatocyte−fibroblast interactions. Importantly, the photoresist removal process consisting of a brief acetone incubation and sonication was found to have no detrimental effects on the ability of several common ECM proteins (collagens I, II, and IV and laminin) to support hepatocyte cultures. The merging of photoresist lithography and robotic protein printing described here allows us to encode different scenarios of cell−cell interactions into printed protein arrays. This approach will be particularly useful for the investigation of scarce and difficult-to-culture cells where a small number of cells seeded into a single culture dish will be exposed to multiple scenarios of cell−cell and cell−surface interactions.

Experimental Section

Chemicals and Materials. Glass slides (75 × 25 mm) were obtained from VWR International. 3-Acryloxypropyl trichlorosilane was purchased from Gelest, Inc. Sulfuric acid, hydrogen peroxide, ethanol, acetone, Tween-20, collagen from rat tail (type I), collagen from chicken sternal cartilage (type II), fibronectin from human plasma, laminin from Engelbreth−Holm−Swarm murine sarcoma basement membrane, and monoclonal antibodies for anti-human albumin, anti-collagen type I, and anti-fibronectin produced in mouse were obtained from Sigma−Aldrich. Human fibronectin was obtained from Chemicon International Inc. Goat anti-mouse IgG2a, Texas Red-conjugated, and goat anti-mouse IgG, fluorescein isothiocyanate (FITC) conjugated, were purchased from Santa Cruz Biotechnologies, Inc. Phosphate-buffered saline (PBS) 10× was purchased from Cambrex. Dulbecco's modified Eagles' medium (DMEM), minimal essential medium (MEM), sodium pyruvate, nonessential amino acids, fetal bovine serum (FBS), FITC-labeled collagen type I, 4′,6-diamidino-2-phenylindole, dilactate (DAPI, dilactate) and Alexa Fluor 555 monoclonal antibody labeling kit were purchased from Invitrogen Life Technologies. FluoroLink Cy3 reactive dye 5-pack was purchased from Amersham Bioscience. Goat anti-human albumin antibody was obtained from Bethyl Laboratories, Inc. Streptavidin−horseradish peroxidase (HRP) was obtained from BD Biosciences. Goat anti-human albumin antibody, goat anti-human albumin antibody−peroxidase conjugate, and reference serum were obtained from Bethyl Laboratories, Inc. The human hepatoblastoma cells, HepG2, were obtained from the American Type Culture Collection.

Surface Modification. Glass slides were cleaned by immersion for 10 min in piranha solution consisting of three parts of sulfuric acid (95% v/v in water) and one part hydrogen peroxide (35% w/v in water). Glass slides were then thoroughly rinsed with deionized (DI) water, dried under nitrogen, and kept in a class 1000 clean room at room temperature. Prior to silane modification, the glass slides were treated in an oxygen plasma chamber (YES-R3, San Jose, CA) at 300 W for 5 min. For silane modification, glass substrates were placed in 2 mM solution of 3-acryloxypropyl trichlorosilane diluted in anhydrous toluene for 10 min. The reaction was performed in a glove box under nitrogen purge to eliminate atmospheric moisture. After modification, the slides were rinsed with fresh toluene, dried under nitrogen, and cured at 100 °C for 2 h. Contact angle measurements (Rame-Hart goniometer) were routinely performed to assess quality of silane modification. In addition, silane assembly and subsequent collagen deposition were investigated by ellipsometry (LSE Stokes ellipsometer, Gaertner Scientific). In these experiments, 4 in. silicon wafers (Wafer World) were diced into smaller pieces (0.5 × 0.5 in.) and modified by procedures identical to those described for glass substrates. Presence of the silane layer was determined by ellipsometry, with optical constants obtained from the same substrate prior to silanization. The silane-modified surfaces were incubated with 0.2 mg/mL solution of collagen I in 1× PBS for 30 min at room temperature. The thickness of assembled protein layer was measured by use of optical constants obtained for the clean Si substrate, with the refractive index taken to be 1.45. Ellipsometry measurements from at least three regions of the same substrate were collected to obtain an average thickness for each sample. The number of samples tested was $n = 3$.

Photoresist Lithography and Microarray Printing. AZ 5214-E positive photoresist was spin-coated on a silane-modified glass substrate at 800 rpm for 10 s followed by 4000 rpm for 30 s. The coated slide was soft-baked on a hot plate at 100 °C for 85 s. The photoresist layer was exposed to UV light (10 mW/cm^2) for 35 s by use of a Canon PLA-501F mask aligner. The exposed photoresist was then developed for 5 min in AZ 300 MIF developer solution,

(22) Schena, M.; Shalon, D.; Davis, R. W.; Brown, P. O. *Science* **1995**, *270*, 467−470.
(23) Revzin, A.; Rajagopalan, P.; Tilles, A. W.; Berthiaume, F.; Yarmush, M. L.; Toner, M. *Langmuir* **2004**, *20*, 2999−3005.
(24) Lee, K. B.; Park, S. J.; Mirkin, C. A.; Smith, J. C.; Mrksich, M. *Science* **2002**, *295*, 1702−1705.
(25) Lynch, M.; Mosher, C.; Huff, J.; Nettikadan, S.; Johnson, J.; Henderson, E. *Proteomics* **2004**, *4*, 1695−1702.
(26) Moran-Mirabal, J. M.; Tan, C. P.; Orth, R. N.; Williams, E. O.; Craighead, H. G.; Lin, D. M. *Anal. Chem.* **2007**, *79* (3), 1109−1114.
(27) Javazon, E. H.; Colter, D.; Schwartz, E. J.; Prockop, D. J. *Stem Cells* **2001**, *19*, 219−225.
(28) Purpura, K. A.; Aubin, J. E.; Zandstra, P. W. *Stem Cells* **2003**, *22*, 39−50.
(29) Nakamura, T.; Yoshimoto, K.; Nakayama, Y.; Tomita, Y.; Ichihara, A. *Proc. Natl. Acad. Sci. U.S.A.* **1983**, *80*, 7229−7233.

briefly washed with DI water to remove residual developing solution, and then dried under nitrogen.

All proteins were dissolved in 1× PBS containing 0.005% Tween-20 at 0.2 mg/mL concentration. Protein microarrays were contact-printed under ambient conditions on photoresist-patterned glass slides using a MicroCaster hand-held microarrayer system (Whatman Schleicher&Schuell) or GMS 417 robotic arrayer (Genetic Micro Systems, Inc.). The individual protein spots printed with MicroCaster instrument were 500 μm in diameter, while the spots generated by GMS 417 arrayer were 300 μm in diameter. The micropatterned glass substrates were sonicated in acetone for 10 min to remove the photoresist and then rinsed with DI water and dried under nitrogen. Glass slides containing protein arrays were kept in a refrigerator for at least 1 month without detrimental effects to cell attachment.

Characterization of Protein Micropatterns. The quality of protein arrays was assessed by fluorescent labeling of proteins prior to printing or by immunostaining after the printing process. Collagen I and fibronectin were conjugated with fluorescein isothiocyanate (FITC) and Alexa 555 dyes, respectively, according to the manufacturer's instructions.[30] For immunofluorescent staining of ECM protein spots, samples were blocked with 1% bovine serum albumin (BSA) by incubation for 0.5∼1 h. The primary antibody solution (antibody for collagen I or fibronectin, dilution ratio 1:2000) was added and incubated for 1 h. Then the secondary antibody solution (anti-mouse IgG, FITC-conjugated, dilution ratio 1:100) was added and the mixture was incubated for 1 h. The samples were then dried under nitrogen and observed under a LSM 5 Pascal confocal microscope (Carl Zeiss Inc). All incubations were performed at room temperature and the samples were washed with 1× PBS three times for 5 min between incubation steps.

AFM images were obtained by use of an MFP-3D (Asylum Research). The 3D motion assembly was equipped with a nanopositioning sensor that monitors piezotranslator motion to correct for piezo creeping and hysteresis. The AFM scanner is mounted on an inverted optical microscope (Olympus IX 81), which allows visualization of protein microarrays and guidance of the AFM probes to the selected locations for high-resolution imaging. A Si cantilever (Olympus AC240TS) with a force constant of $k = 2.0$ N/m was used for AFM imaging under ambient conditions. Noncontact mode imaging was utilized for visualizing these microstructures with a typical resonance frequency of 40.1 kHz and 95% damping ratio.

Formation of Cellular Micropatterns. HepG2 cells were maintained in MEM supplemented with 10% FBS, 200 units/mL penicillin, 200 μg/mL streptomycin, 1 mM sodium pyruvate, and 0.1 mM nonessential amino acids at 37 °C in a humidified 5% CO_2 atmosphere. Murine 3T3 fibroblasts were maintained in DMEM supplemented with 10% FBS, 200 units/mL penicillin, and 200 μg/mL streptomycin at 37 °C in a humidified 5% CO_2 atmosphere. Prior to cell seeding, 75 × 25 mm glass slides were cut into 20 × 25 mm glass pieces with a diamond scribing pen, sterilized with 70% ethanol, and washed with 1× PBS twice.

For cell seeding experiments, glass pieces were placed into wells of a conventional 6-well plate. To create micropatterned mono- and cocultures, collagen-patterned slides were first exposed to 3 mL of HepG2 cell suspension in culture medium at a concentration of 1×10^6 cells/mL. After 1 h of incubation at 37 °C, the medium containing unattached cells was removed and surfaces were washed twice with 1× PBS. To introduce the second cell type, glass slides containing surface-bound arrays of HepG2 cells were exposed to 3 mL of fibroblast cell suspension at a concentration of 2.5×10^5 cells/mL. After incubation at 37 °C for 20 min, the fibroblast culture medium was removed and replaced with HepG2 culture medium. Cell arrays formed on the glass slide were imaged by use of bright-field microscopy (Zeiss Axiovert 40, Carl Zeiss Inc.).

Intracellular staining for albumin was carried out in order to characterize hepatic function. Prior to immunohistochemical staining, micropatterned cell cultures were washed three times in prewarmed (37 °C) 1× PBS, were fixed with 4% paraformaldehyde for 15 min, and then permeabilized in 0.1% aqueous solution of Triton X-100 for 5 min. The cells were then incubated in 1% bovine serum albumin (BSA) in 1× PBS for 1 h to diminish nonspecific staining and incubated with 1:1000 diluted biotinylated anti-human albumin antibody overnight at 4 °C. Finally, micropatterned cell cultures were incubated in 1:1000 diluted HRP-conjugated streptavidin for 2 h followed by color developing with diaminobenzidine (DAB). Between steps in the process, the cells were washed three times for 5 min with 1× PBS. Stained cells were visualized and imaged by bright-field microscopy.

Counting the Number of Cells Attached on Micropatterned Protein Arrays. Micropatterned cells were fixed on the surface by incubating in acetone for 5 min and then stained with DAPI, a DNA-binding fluorophore that stains the nucleus. Stained cells were characterized and counted on a laser scanning cytometer (CompuCyte Corp., Cambridge, MA). The samples were mounted on a stage and characterized by use of an argon laser at 488 nm and helium−neon laser at 633 nm. All analyses were carried out with a 20× objective. The arrays of interest were sequentially scanned with both lasers, generating a pixel-to-pixel map of the cells. The acquired data were displayed and analyzed with WinCyte software (CompuCyte Corp., Cambridge, MA). It generated a dot plot of the x and y positions of all the cells in the arrays. Arrays of interest were manually chosen and the software provided information about the number of cells in these arrays. The cells attached to micropatterned protein arrays with encoded dimensions of 30, 50, 100, and 200 μm were enumerated. In each sample, cells on 20 protein spots (500 μm diameter) encoded with attachment sites of specific dimensions were counted. The number of samples was $n = 3$.

Investigating the Effects of Photoresist Lift-off on Protein Arrays. Several ECM proteins (collagens I, II, and IV and laminin) were selected in order to study the effects of acetone treatment on the ability of protein arrays to support adhesion and function of hepatocytes. Printed protein arrays underwent treatment, identical to photoresist lift-off, and consisting of sonication in acetone for 10 min followed by washing with DI water. HepG2 cells were then seeded onto acetone-treated and nontreated protein arrays. For quantifying the number of attached cells, protein arrays were incubated with HepG2 cells for 4 h, fixed in acetone, stained with a nucleus (DNA)-specific fluorophore DAPI, and then imaged via fluorescence microscopy. The captured images were processed with ImageJ software to calculate the average number of nuclei in cells residing on protein spots. For each protein type, hepatic cells residing on at least six protein spots (500 μm diameter) were counted. The hepatic function of HepG2 cells cultured on acetone-treated and nontreated protein arrays was monitored by collecting culture medium daily for 7 days. Collected culture medium was analyzed for albumin secretion by a standard enzyme-linked immunosorbent assay (ELISA) method described earlier.[23] For each protein type, albumin assay was performed on at least three ($n = 3$) surfaces containing cellular micropatterns.

Results and Discussion

In this study, protein microarraying was combined with photoresist lithography to create cell culture surfaces where cell−ECM and cell−cell interactions can be defined in a precise and multiplexed manner. In the future, such combinatorial cell culture systems will be used to expedite discovery of the microenvironment niche required for induction of tissue-specific function in stem cells or for maintenance of differentiated phenotype in scarce primary cells.

Creating Micropatterned Protein Arrays. The ECM proteins constitute a major component of cellular microenvironment and are responsible for guiding cell attachment, providing signals for tissue morphogenesis and induction of tissue-specific differentiation.[31−34] While this study investigated the possibility of creating micropatterned arrays of several ECM proteins,

(30) *Handbook of Fluorescent Probes and Research Chemicals*, 6th ed.; Molecular Probes: Eugene, OR, 1996.

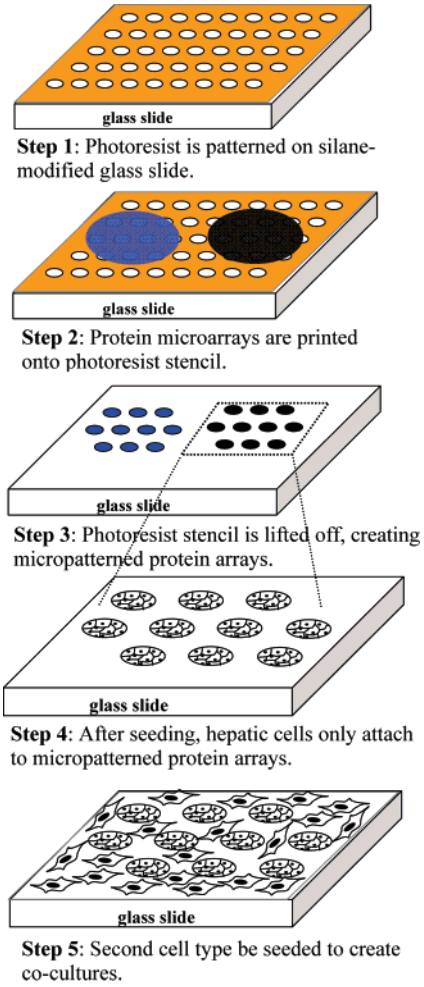

Figure 1. Diagram describing surface micropatterning procedure. (Step 1) Positive photoresist is micropatterned on silane-modified glass slides. Silane modification ensures selective attachment of hepatic cells to protein domains. (Step 2) Arrays consisting of multiple proteins are printed onto the photoresist stencil. (Step 3) Photoresist is removed by brief sonication in acetone (lift-off procedure), creating micropatterned protein arrays. (Step 4) Hepatic cells seeded onto the surface attach to ECM protein domains but not to silane-modified regions of the glass substrate. (Step 5) Secondary cells (fibroblasts) attach on silane-modified regions of the substrate, forming hepatocyte−fibroblast cocultures on micropatterned protein arrays.

collagen I was employed in the majority of cell micropatterning studies due to its extensive use with hepatocyte cultures.[33,34]

The surface patterning process developed in this paper is described diagrammatically in Figure 1. This process employs a photoresist layer as a stencil during the printing of protein microarrays. Because both photoresist and protein microarray patterns are periodic, no alignment is required for their superimposition. The robotic protein printing is advantageous for presenting multiple biomolecules on the surface and for investigation of cell−surface interactions in a multiplexed fashion,[5,6] however, the dimensions and geometry of the printed spot are largely driven by the design of the printing pin. For most pin designs this leads to printing of circular spots with diameter in a 100−500 μm range. Given that the size of mammalian cells varies from 5 to 20 μm in diameter, printed protein spots accommodate clusters of 20−300 cells and do not offer precise control over cell−cell interactions.

While a positive photoresist layer was employed as a temporary stencil during printing of protein arrays in this study, other materials such as silicone rubber[35,36] or Parylene[26] may be used as stencils for patterning biomolecules on surfaces. In comparison to Parylene, patterning and processing of photoresist is considerably simpler. While silicone rubber stencils are easy to fabricate, handling and securing these membranes onto substrates of large surface area (e.g., 75 × 25 mm glass slides) may not be trivial. On the basis of considerations of simplicity of patterning and handling, we chose to employ standard positive photoresist as a stencil for printing protein microarrays.

As shown in Figure 2A, use of a microfabricated photoresist layer allowed us to create a stencil with micrometer-scale lateral dimensions on a glass substrate. Printing of protein arrays onto glass slides containing photoresist patterns, followed by photoresist removal (lift-off), resulted in formation of micropatterned protein arrays shown in Figure 2B−E. As seen from these images, the photoresist stencil allowed us to decouple geometry and dimensions of the cell attachment sites from the overall dimensions of the printed protein spots. While the printed spots were 500 μm in diameter, the area of cell attachment sites varied from 30 μm diameter regions suitable for accommodating individual cells (Figure 2B) to 50 and 100 μm diameter regions that were expected to support attachment of multiple cells (Figure 2C,D). Figure 2E underscores the possibility of printing multiple ECM proteins while exercising precise control over the dimensions encoded into protein spots. In this experiment, collagen I−FITC (green) and fibronectin−Alexa 555 (red) were robotically printed onto a glass substrate containing a periodic pattern of 30 μm diameter wells fabricated in photoresist. After photoresist removal by acetone sonication, the surface contained 300 μm diameter protein spots of collagen I and fibronectin with each spot subdivided into 30 μm diameter domains (Figure 2E). Importantly, the features encoded into protein spots are controlled by the photomask design and the photoresist resolution. The ability to vary lateral dimensions of the protein features from one printed spot to another, coupled with the ability to print multiple ECM in the same microarray, provides the potential to orchestrate cell−cell and cell−ECM interaction scenarios in a combinatorial fashion.

It should be noted that micropatterned domains of collagen I (Figure 2B−D) and fibronectin (data not shown) stained positive during immunofluorescent labeling experiments. This demonstrated that the protein molecules retained antibody-binding epitopes after organic solvent exposure and were not fully denatured in the course of the lift-off process. Another interesting observation is a degree of heterogeneity in fluorescence signal observed in Figure 2E, where collagen I−FITC and fibronectin−Alexa 555 were printed side-by-side. This observation contrasts with Figure 2B−D showing uniform distribution of immunofluorescently stained micropatterned collagen I spots. Given that the same proteins was used in both cases, the heterogeneity seen in Figure 2E may be attributed to changes in physicochemical properties of proteins due to or in the process of fluorescent labeling.

(31) Werb, Z.; Chin, J. R. *Ann. N.Y. Acad. Sci.* **1998**, *857*, 110−8.
(32) Lelievre, S. A.; Weaver, V. M.; Nickerson, J. A.; Larabell, C. A.; Bhaumik, A.; Petersen, O. W.; Bissell, M. J. *Proc. Natl. Acad. Sci. U.S.A.* **1998**, *95*, 14711−6.
(33) Berthiaume, F.; Moghe, P. V.; Toner, M.; Yarmush, M. L. *FASEB J.* **1996**, *10*, 1471−1484.
(34) Ben-Ze'ev, A.; Robinson, G. S.; Bucher, N. L. R.; Farmer, S. R. *Proc. Natl. Acad. Sci. U.S.A.* **1988**, *85*, 2161−2165.
(35) Folch, A.; Jo, B.-H.; Hurtado, O.; Beebe, D. J.; Toner, M. *J. Biomed. Mater. Res.* **2000**, *52*, 346−353.
(36) Jackman, R. J.; Duffy, D. C.; Cherniavskaya, O.; Whitesides, G. M. *Langmuir* **1999**, *15*, 2973−2984.

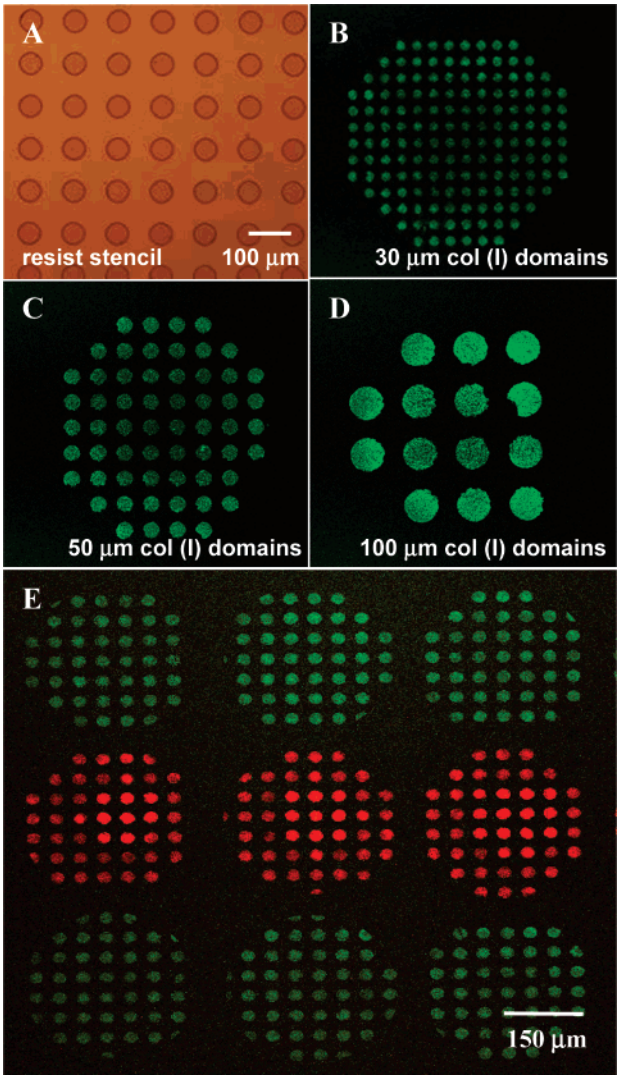

Figure 2. Creating micropatterns within printed protein spots. (A) Photoresist stencil consisting of 50 μm diameter circles. (B−D) Collagen I spots (500 μm diameter) were printed over a photoresist stencils consisting of (B) 30, (C) 50, and (D) 100 μm diameter circles. After the lift-off process, collagen spots retained features encoded by photolithography. The surfaces containing protein patterns were incubated with primary anti-rat collagen antibodies followed by FITC-labeled secondary antibody. (E) Fluorescence images of arrays of 300 μm diameter protein spots [collagen I−FITC and fibronectin−Alexa 555] robotically printed over a photoresist stencil. Micropatterns within collagen and fibronectin spots consist of 30 μm diameter protein features. Photoresist was removed prior to imaging.

Characterization of Protein Micropatterns. Characterization of the morphology and topography of the micropatterns of collagen I was carried out by AFM. As shown in Figure 3, printing of collagen I over a photoresist stencil composed of 30 μm diameter features led to formation of collagen disks with diameter of 29.0 ± 0.5 μm. The height of these disks was 3.0 ± 1.0 nm, as revealed from the cursor profile in Figure 3A. The AFM topograph displayed in 2D and 3D in conjunction with the cursor plot also reveals the presence of a thin (1.8 nm) and tall (6 nm) boundary of each disk. The formation of such boundary is likely due to the conformal coating of the protein over the exposed and photoresist-protected regions of the glass substrate. This conformal coating might have resulted in formation of a thicker collagen layer next to the walls of the photoresist pattern. The difference in thickness between the edge and center of collagen pattern was likely retained after photoresist removal.

On the basis of the dimensions of individual triple-helical collagen I molecules (1.5 nm in width and 300 nm in length),[37] the 3.0 ± 1.0 nm layer measured by AFM points to the presence of monomeric collagen one or two layers thick. Our ellipsometric studies of collagen adsorption onto acrylated silane-modified Si substrates yielded thickness of 4.9 ± 0.4 nm, corroborating the AFM measurements. The supramolecular organization of collagen into fibrils has been shown to be promoted by elevated (37 °C) temperatures, surface hydrophobicity of substrata, and adsorption times.[38−40] Our experiments were carried out at room temperature, with small volumes (1−50 nL) of protein solution robotically dispensed onto substrates of moderate hydrophobicity (∼55° contact angle). This process likely resulted in rapid evaporation of solvent and adsorption of a thin monomeric collagen layer. Our AFM and ellipsometry results are consistent with previous reports of organization of monomeric collagen I layers on surfaces.[18,39]

Micropatterning Hepatic Cells on Protein Arrays. Cell−cell interactions have been demonstrated to play an important role in maintainenance of differentiated hepatic phenotype. Ben-Ze'ev et al.[34] demonstrated a shift toward proliferation program in sparsely seeded hepatocytes. Conversely, increasing the seeding density resulted in upregulation of hepatic gene expression and function. This density-dependent regulation of proliferation or differentiation programs in hepatocytes has been attributed to presence of "cell surface modulators" (juxtacrine signaling) controlling cellular fate through contact[29,41] but may also be due to short-range endocrine signaling.

Given the importance of cell−cell interactions in defining cellular phenotype, we wanted to develop a micropatterning strategy allowing us to superimpose multiple scenarios of cell−cell contacts (i.e., single cells vs small vs larger cell clusters) onto protein microarrays to enable multifactorial investigation of cell−cell and cell−substrate interactions. As demonstrated in Figure 4, the photolithography technique offers excellent control of cell−cell contacts occurring on robotically printed protein spots. Figure 4A shows a typical cluster of hepatic cells attaching onto a 500 μm diameter collagen I spot. While the design of the surface properties ensures that hepatic cells are localized to a protein domain, the extent of "on-the-spot" intercellular contacts is poorly defined with ∼300 cells formed into a cluster. When seeded onto surfaces patterned by the combination of protein printing and photoresist lithography, HepG2 cells retained preference for attachment to collagen I domains; however, as seen from Figure 4B−H, the extent of "on-the-spot" cell−cell contacts was now well-defined.

In order to ascertain the extent of cell−cell contacts created on the attachment sites of different dimensions, the micropatterned hepatic cells were stained a DNA-selective fluorophore DAPI and enumerated by laser scanning cytometry. Quantification of the number of cells occupying attachment sites of different dimensions (Figure 4B) revealed that 30 μm diameter domains sequestered 1.34 ± 0.61 cells while 50 μm diameter regions contained 5.4 ± 1.3 cells. Increasing the diameter of photolithographically defined features to 100 and 200 μm resulted in attachment of 21 ± 2.8 and 77 ± 13.2 cells, respectively. Further

(37) Piez, K. A.; Reddi, A. H. *Extracellular Matrix Biochemistry*; Elsevier: New York, 1984.
(38) Elliott, J. T.; Tona, A.; Woodward, J. T.; Jones, P. L.; Plant, A. L. *Langmuir* **2003**, *19*, 1506−1514.
(39) Denis, F. A.; Hanarp, P.; Sutherland, D. S.; Gold, J.; Mustin, C.; Rouxhet, P. G.; Dufrene, Y. F. *Langmuir* **2002**, *18*, 819−822.
(40) Pamula, E.; De Cupere, V.; Dufrene, Y. F.; Rouxhet, P. G. *J. Colloid Interface Sci.* **2004**, *271*, 80−91.
(41) Nakamura, T.; Nakayama, Y.; Teramoto, H.; Nawa, K.; Ichihara, A. *Proc. Natl. Acad. Sci. U.S.A.* **1984**, *81*, 6398−6402.

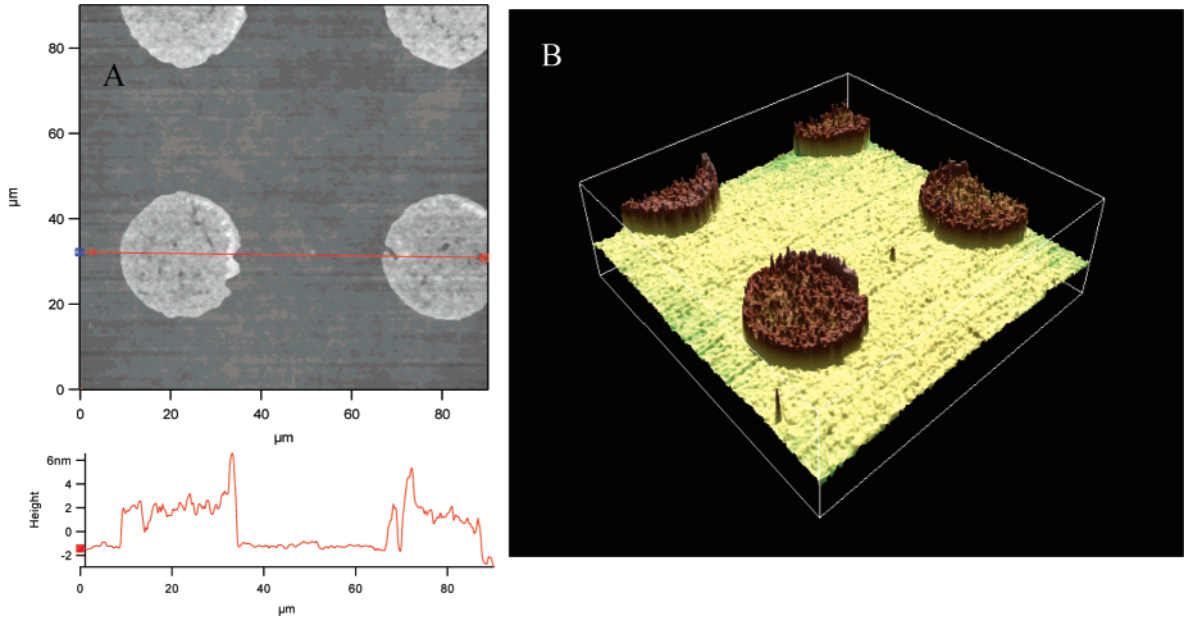

Figure 3. AFM characterization of collagen micropatterns. The total scanning area is 90 × 90 μm^2, with a scanning speed of 0.1 Hz. (A) AFM topograph and corresponding cursor profile revealed three-dimensional collagen microdiscs. The vertical scale is 19 nm. (B) Three-dimensional view of the image shown in panel A allows to visualize spot morphology.

characterization was performed to analyze the distribution of cell cluster sizes formed on protein attachment sites of different dimensions. These results demonstrate that hepatic micropatterns formed on 30 μm domains (Figure 4C,D) were largely composed of single cells (50% of cases) with lower frequency of occurrence of two- and three-cell clusters (19% of cases). A large number (30%) of "unoccupied" sites may point to 30 μm domains not providing sufficient area for attachment of larger cells within the population interacting with the micropatterned surface. As seen from Figure 4E,F, the hepatocytes residing on 50 μm domains were organized into clusters of 5−6 cells (~60% of cases) whereas larger clusters of 20−23 cells were observed most frequently (~60% of cases) on 100 μm diameter domains (Figure 4G,H). Importantly, all three scenarios were created within protein microarrays printed on the same surface. The data presented in Figure 4 further underscore the tight control over the extent of cell−cell contacts that can be achieved by photolithographic patterning of printed protein spots.

Formation of Co-cultures on Micropatterned Protein Arrays. In addition to defining interactions between the cells of the same type (homotypic interactions), there is considerable interest in creating cultures consisting of two or more cell types in order to orchestrate heterotypic interactions.[18,42,43] Co-cultures are thought to be better mimics of the in vivo microenvironment where multiple cell types interact and influence each other in a reciprocal fashion. For example, co-cultivation of primary hepatocytes with nonparenchymal cells of liver or nonliver origin has been shown to extend and enhance expression of liver-specific function in these cells.[42,44] Photoresist lithography was previously employed by Bhatia et al.[18,44] to create microfabricated hepatocyte cocultures where the location of two cells types and the extent of homotypic and heterotypic interactions could be controlled in a precise and reproducible fashion.

Given the importance of co-cultures in cultivation of hepatocytes, we investigated the possibility of adding another cell type to the hepatic cells adherent on the micropatterned protein arrays. While different methods have been employed to ensure spatial localization of cells in micropatterned cocultures,[18,23,45] we found that glass substrates modified with acrylated silane (acryloxypropyl trichlorosilane) were temporarily resistant to attachment of hepatocytes while allowing attachment of nonparenchymal cells such as 3T3 fibroblasts or stellate cells. This selectivity in adhesion of different cell types is driven, at least in part, by the optimization of cell seeding protocols for each cell type, the ability of the cells to modify their environment by secreting endogenous ECM molecules, and the intrinsic properties of the surface (e.g., wettability and free surface energy).[46] Figure 5A demonstrates that the addition of 3T3 fibroblasts to the hepatocytes micropatterned on collagen I protein spots resulted in formation of spatially defined co-cultures. After 2 days in culture, fibroblasts proliferated and occupied all of the surface area between the hepatic clusters as shown in Figure 5B. Immunostaining experiments were carried out (see Figure 5C) to identify albumin-producing hepatic cells within the cocultures and to demonstrate a potential method for delineating the effects of local microenvironment on the tissue-specific function of hepatocytes. Figure 5C, depicting cellular micropatterns after 2 days in co-culture, demonstrates that the production of albumin was localized to the hepatic cell clusters within the coculture. In the future, when combinations of cell−surface and cell−cell interactions orchestrated on the same glass slide will be expected to induce expression of different levels of liver function across the same slide, intracellular staining for liver-specific proteins may be used to identify the optimal microenvironment conditions. Another prospective method to analyze liver-specific function without losing the local microenvironment context has been demonstrated by us recently.[47] This approach consisted of retrieval of hepatic cells from selected locations within the microfabricated cell cultures by laser microdissection followed by the analyses of liver-specific gene expression by reverse transcriptase (RT)−

(42) Corlu, A.; Ilyin, G.; Cariou, S.; Lamy, I.; Loyer, P.; Guguen-Guillouzo, C. *Cell Biol. Toxicol.* **1997**, *13*, 235−242.
(43) Zinchenko, Y. S.; Coger, R. N. *J. Biomed. Mater. Res. A* **2005**, *75*, 242−248.
(44) Bhatia, S. N.; Balis, U. J.; Yarmush, M. L.; Toner, M. *FASEB J.* **1999**, *13*, 1883−1900.
(45) Khademhosseini, A.; Suh, K. Y.; Yang, J. M.; Eng, G.; Yeh, J.; Levenberg, S.; Langer, R. *Biomaterials* **2004**, *25*, 3583−3592.
(46) Krasteva, N.; Groth, T. H.; Fey-Lamprecht, F.; Altankov, G. *J. Biomater. Sci., Polym. Ed.* **2001**, *12*, 613−27.
(47) Lee, J. Y.; Jones, C. N.; Zern, M. A.; Revzin, A. *Anal. Chem.* **2006**, *78*, 8305−8312.

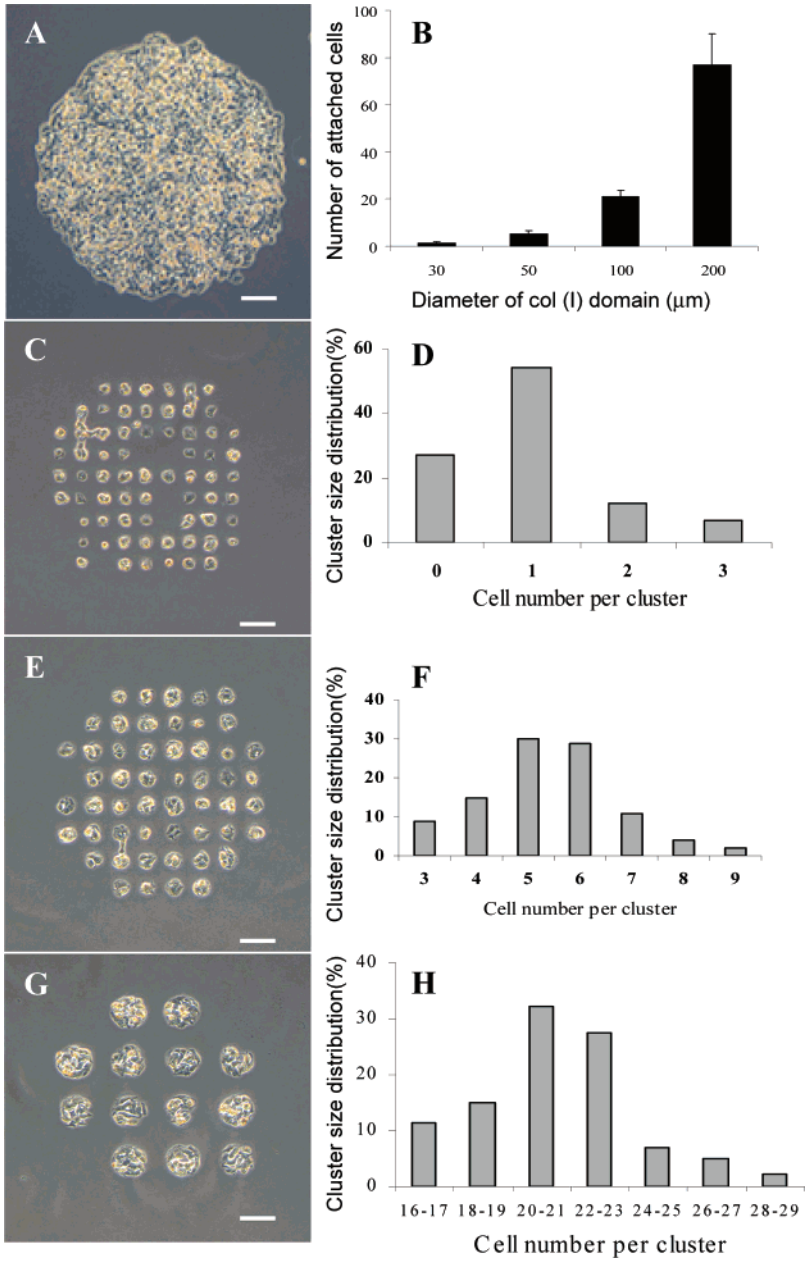

Figure 4. Control over cell−cell contacts in hepatic (HepG2) cells seeded onto micropatterned protein spots. Error bar corresponds to 100 μm. (A) Cluster of ~300 HepG2 cells attached to a single 500 μm collagen I spot. The intercellular contacts of cells residing on the spot are not defined. (B) Quantification of cells residing on attachment sites of different areas: 30 μm diameter features 1.3 ± 0.6 cells; 50 μm diameter features 5.4 ± 1.3 cells; 100 μm diameter features 21 ± 2.8 cells; and 200 μm diameter features 77 ± 13.2 cells. (C, D) HepG2 cells attached on 30 μm diameter features encoded into 500 μm diameter collagen I spot. Single cells were observed in over 50% of cases. (E, F) Hepatic cells attaching on 50 μm diameter domains defined within 500 μm diameter collagen I spot. The frequency of formation of small clusters of 5−6 cells was ~60%. (G, H) Hepatic cells residing on 100 μm domains formed larger clusters of 20−23 cells in ~60% of cases.

polymerase chain reaction (PCR). In addition to being more quantitative, RT-PCR-based analysis allows to monitor larger numbers of markers associated with liver-specific phenotype.

Investigating the Effects of Photoresist Lift-off Process on Protein Arrays. The surface modification process leading to the formation of micropatterned protein arrays employed the standard lift-off procedure for removal of the photoresist after protein printing. The lift-off procedure required a brief (10 min) immersion of the photoresist/protein pattern in acetone combined with sonication. Given the potential for protein denaturation due to organic solvent exposure, experiments were carried out to characterize micropatterned surfaces.

Beyond immunofluorescent staining experiments presented in Figure 2B−D, studies were undertaken to investigate the effects of the lift-off process on the ability of protein arrays to support hepatocyte attachment and function. In these studies, arrays of representative ECM proteins (collagens I, II, and IV and laminin) printed on glass substrates were exposed to lift-off conditions (acetone and sonication) and incubated with HepG2 cells. The protein microarrays not exposed to organic solvent served as controls. Figure 6A compares the numbers of cells adherent on acetone-treated and nontreated protein arrays. In these experiments, HepG2 cells were incubated with the micropatterned surfaces for 4 h, stained with the DNA-selective fluorophore DAPI, and quantified. As seen from Figure 6A, the lift-off process had no deleterious effects on cell attachment as both acetone-treated and nontreated protein arrays supported adhesion of HepG2 cells.

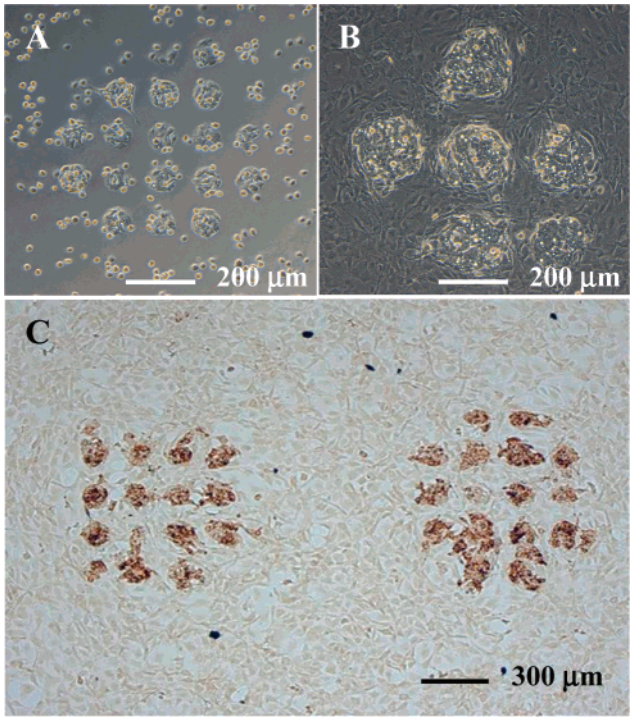

Figure 5. Creating hepatocyte−fibroblast cocultures on micropatterned protein spots. (A) 3T3 fibroblasts 1 h after seeding onto a surface containing micropatterned hepatic cells. HepG2 cells were cultured on 100 μm diameter collagen pattern. (B) Micropatterned cocultures formed on 200 μm diameter collagen I domains 2 days after fibroblast seeding. (C) Immunohistochemical staining of cocultures for intracellular albumin. Signal due to HRP is specific to 100 μm diameter HepG2 clusters within the coculture.

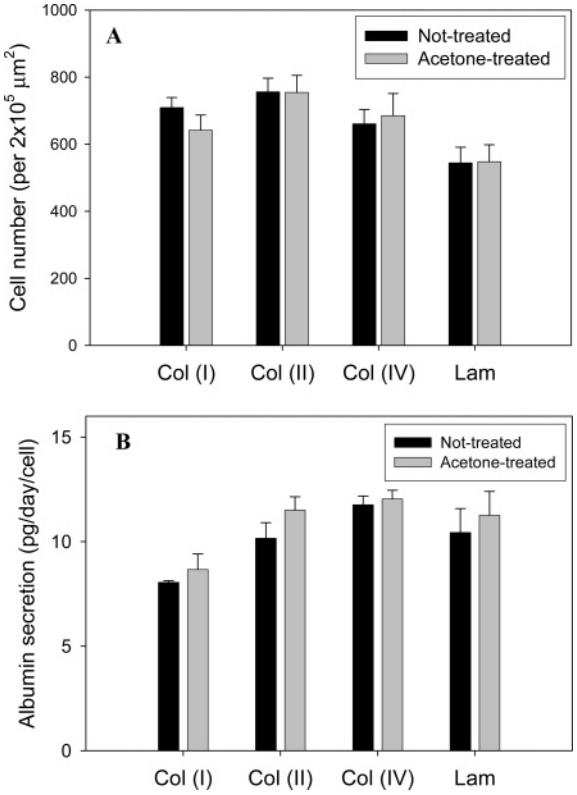

Figure 6. Investigating attachment and function of hepatic cells on protein arrays exposed to organic solvent. Redundant arrays of one protein type printed on the glass substrates were exposed to acetone and incubated with HepG2 cells. Nontreated arrays of the same protein type were used as controls. (A) Analysis of the number of hepatic cells attached on protein spots after 4 h of incubation. No significant difference was observed in the number of cells adherent on acetone-treated and nontreated protein arrays. At least six cell clusters formed on 500 μm diameter protein spots (~1800 cells) were counted for each condition. Statistical analysis was performed by paired *t*-test, with probability values of less than 0.05 considered statistically significant. (B) Hepatic function of HepG2 cells cultured on acetone-treated and nontreated protein spots was monitored by albumin ELISA. The results for albumin secretion at day 4 in culture show no significant difference in albumin levels between acetone-treated and nontreated ECM proteins. For each condition, albumin secretion was analyzed for at least three samples ($n = 3$). Statistical analysis was performed by paired *t*-test, with probability values of less than 0.05 considered statistically significant.

In order to investigate longer-term effects of the lift-off process, HepG2 cells were cultured for 7 days on acetone-treated and nontreated arrays of four representative ECM proteins. The hepatic function was monitored by albumin ELISA and cell morphology was observed by bright-field microscopy. As seen from Figure 6B, showing results from day 4 of cell culture, albumin synthesis of HepG2 cells cultured on acetone-treated protein arrays was comparable to nontreated arrays for all four proteins tested. No differences in albumin secretion between the acetone-treated and nontreated surfaces were noticed at other time points. Overall, the evidence presented here points to compatibility of our surface micropatterning strategy with multiple ECM proteins.

Conclusions

The present paper describes a novel micropatterning strategy for designing complex cell−ECM protein and cell−cell interactions. The merger of traditional photoresist lithography with robotic protein printing allowed us to encode micrometer-scale cell-adhesive domains within 300 or 500 μm diameter protein spots. The micropatterned glass surfaces were engineered to allow for selective attachment of hepatoma (HepG2) cells onto protein domains and adhesion of 3T3 fibroblasts elsewhere on the glass surface. Importantly, the photoresist lift-off process did not have deleterious effects on hepatocyte attachment and function on protein arrays. Overall, the proposed micropatterning approach offers the potential to develop novel cell culture substrates for screening multiple scenarios of cell−microenvironment interactions in parallel. These cell culture substrates will utilize ECM protein arrays to study cell−matrix interactions and photolithography to orchestrate multiple scenarios of intercellular contacts within the ECM protein spots. The micropatterned protein surfaces described here are envisioned as cell culture tools enabling high-throughput discovery of the microenvironment niche for induction of tissue specification in stem cells or maintenance of differentiated phenotype in scarce primary cells.

Acknowledgment. We thank Dr. Angelique Louie from the Department of Biomedical Engineering at UC Davis for use of the confocal microscope. We also thank Ms. Caroline Jones from the Department of Biomedical Engineering at UC Davis for assistance with cell culture and surface characterization experiments. Financial support for this work was provided by the National Institutes of Health (DK073901) and by UC Davis start-up funds.

LA702883D